Elastic Proton-Proton Scattering at 90° and Structure within the Proton*

C. W. AKERLOF, R. H. HIEBER, A. D. KRISCH
Randall Laboratory of Physics, University of Michigan, Ann Arbor, Michigan

AND

K. W. EDWARDS†
Department of Physics, University of Iowa, Iowa City, Iowa

AND

L. G. RATNER
Particle Accelerator Division, Argonne National Laboratory, Argonne, Illinois

AND

K. RUDDICK‡
Department of Physics, University of Minnesota, Minneapolis, Minnesota

(Received 3 January 1964)

The differential cross section for proton-proton elastic scattering at 90° in the center-of-mass system was measured at laboratory momenta ranging from 5.0 to 13.4 GeV/c. Fifty-one measurements were made at momentum intervals of 100 or 200 MeV/c. The extracted proton beam of the ZGS impinged upon a CH_2 target. The two scattered protons were detected by two spectrometers consisting of magnets and scintillation counter telescopes in coincidence. The incident beam flux was measured by radiochemical analysis of the CH_2 targets. The experiment showed no evidence for any $S=0$, $T=1$ dibaryon resonances in the 3300–5200-MeV mass range. It also yielded some information about the validity of the statistical model and the analyticity of the scattering amplitude. The most interesting result of the experiment was a sharp break in the fixed-angle cross section. This may be evidence for the existence of two inner regions of the proton with radii 0.51±.02 and 0.34±.02 F.

1. INTRODUCTION

IN recent years there has been considerable interest in the elastic scattering of strongly interacting particles at high energies. Many groups[1–19] have studied πp, kp, $\bar{p}p$, and np elastic scattering at small and intermediate angles. However, because of the small cross sections involved, only in the case of proton-proton elastic scattering could the very high momentum transfer processes be studied. Several experiments have

* Supported by a research grant from the U. S. Atomic Energy Commission.
† Supported by a summer grant from Argonne National Laboratory.
‡ At University of Michigan, Ann Arbor, Michigan during the early stages of the experiment.

[1] K. J. Foley, S. J. Lindenbaum, W. A. Love, S. Ozaki, J. J. Russell, and L. C. L. Yuan, Phys. Rev. Letters **10**, 376, 543 (1963); **11**, 425, 503 (1963).
[2] K. J. Foley, R. S. Gilmore, S. J. Lindenbaum, W. A. Love, S. Ozaki, E. H. Willen, R. Yamada, and L. C. L. Yuan, Phys. Rev. Letters **15**, 45 (1965).
[3] D. Harting, B. Elsner, D. O. Caldwell, A. C. Helmholz, W. C. Middelkoop, B. Zacharov, P. Dalpiaz, S. Focardi, G. Giacomelli, L. Monari, J. A. Beaney, R. A. Donald, P. Mason, L. W. Jones, Nuovo Cimento **13**, 60 (1965).
[4] W. R. Frisken, A. L. Read, H. Ruderman, A. D. Krisch, J. Orear, R. Rubinstein, D. B. Scarl, and D. H. White, Phys. Rev. Letters **15**, 309, 313 (1965).
[5] C. Coffin, N. Dikmen, L. Ettlinger, D. Meyer, A. Saulys, K. Terwilliger, and D. Williams, Phys. Rev. Letters **15**, 838 (1965).
[6] Aachen *et al.* collaboration, Phys. Letters **10**, 248 (1964).
[7] D. E. Damouth, L. W. Jones, and M. L. Perl, Phys. Rev. Letters **11**, 287 (1963).
[8] M. L. Perl, Y. Y. Lee, and E. Marquit; Phys. Rev. **138**, B707 (1965).
[9] M. L. Perl, L. W. Jones, and C. C. Ting, Phys. Rev. **132**, 1252 (1963).
[10] P. J. Duke, D. P. Jones, M. A. R. Kemp, P. G. Murphy, J. D. Prentice, J. J. Thresher, H. H. Atkinson, C. R. Cox, and K. S. Heard, Phys. Rev. Letters **15**, 468 (1965).
[11] A. Helland, C. D. Wood, T. J. Devlin, D. E. Hagge, M. J. Longo, B. J. Moyer, and V. Perez-Mendez, Phys. Rev. **134**, B1079 (1964).
[12] S. W. Kormanyos, A. D. Krisch, J. R. O'Fallon, K. Ruddick, and L. G. Ratner; Phys. Rev. Letters **16**, 709 (1966).
[13] K. J. Foley, R. S. Gilmore, R. S. Jones, S. J. Lindenbaum, W. A. Love, S. Ozaki, E. H. Willen, R. Yamada, and L. C. L. Yuan, Phys. Rev. Letters **14**, 862 (1965).
[14] H. Brody, R. Lanza, R. Marshall, J. Niederer, W. Selove, M. Shocket, and R. Van Bert, Phys. Rev. Letters **16**, 828 and 968 (1966).
[15] A. I. Alikhanov, G. L. Bayatyan, E. V. Brakhman, G. P. Eliseev, Yu. V. Galaktionov, L. G. Landsberg, V. A. Lyubimov, I. V. Sidorov, F. A. Yetch, and O. Ya. Zeldovich, Phys. Letters **19**, 345 (1965).
[16] A. S. Vovenko, B. N. Gus'kov, M. F. Likhachev, A. L. Lyubimov, Yu. A. Matulenko, I. A. Savin, and V. S. Stavinskii, Pisma Redaktsiya **2**, 409, 1965 [English transl.: JETP Letters **2**, 255 (1965)].
[17] W. F. Baker, P. J. Carlson, V Chabaud, A. Lundby E. Michaelis, J. Banaigs, J. Berger, C. Bonnel, J. Duflo, L. Goldzahl, and F. Plouin, in Proceedings of the Oxford International Conference on High Energy Physics, September 1965 (unpublished) and (private communications).
[18] M. N. Kreisler, F. Martin, M. L. Perl, M. J. Longo, and S. T. Powell, Phys. Rev. Letters **16**, 1217 (1966) and thesis by M. N. Kreisler, Stanford University, 1966 (unpublished)
[19] J. L. Friedes, H. Palevsky, R. L. Stearns, and R. J. Sutter, Phys. Rev. Letters **15**, 38 (1965). G. Manning *et al.*, Nuovo Cimento **41**, 167 (1966).

measured p-p elastic scattering at very large angles[20–23] in addition to those at small angles[1,13,24,25] Experiments of this type are the principal means of probing the structure of strongly interacting particles below the level of one F.

In this experiment fifty-one differential cross sections, for proton-proton elastic scattering at 90° in the center-of-mass system, have been measured at the Argonne National Laboratory Zero Gradient Synchrotron (ZGS). The incoming proton momentum ranged from 5.0 to 13.4 GeV/c in steps of 100 or 200 MeV/c. This range corresponded to values of squared four-momentum transfers $-t=2P_{\text{c.m.}}^2$ of 3.9 to 11.7 (GeV/c)^2.

The close spacing of measured points coupled with total errors ranging from 2.9% at 5.0 GeV/c to 7.1% at 13.2 GeV/c resulted in a precision which allowed several interesting conclusions to be drawn.

Section 2 will describe the experimental method, Section 3 will summarize the data, and Sec. 4 is devoted to a discussion of the results.

2. EXPERIMENTAL METHOD

The layout of the experiment is shown in Fig. 3. The slow extracted proton beam of the ZGS impinged upon a 1 in. square CH_2 target. The scattered and recoil protons, which emerged at equal angles in the laboratory, were momentum analyzed by the deflection magnets and detected by the left and right counter telescopes. For each measurement, the left and right C magnets were set to compensate for the change in the laboratory opening angle caused by the energy dependence of the Lorentz transformation. The left and right bending magnets deflected the protons by 9° for momentum analysis. The number of proton-proton elastic scattering events was determined by counting the number of coincidences between the left and right telescopes. The number of protons hitting the CH_2 target was determined by a radiochemical analysis of each target.

A. Proton Beam

The proton beam was extracted by using a "front porch" on the ZGS magnetic field at the appropriate momentum as shown in Fig. 1. The internal beam of $1.0\rightarrow 1.5\times10^{12}$ protons per pulse was accelerated up to the "front porch" and a certain fraction was extracted by allowing the beam to hit a beryllium energy loss target. The remaining beam was then accelerated up to full energy for other experimenters. The extraction efficiency was about 25% and the machine repetition rate ranged from $2.2\rightarrow 3.0$ sec. A uniform beam spill of 150 msec was used at each of the desired energies. The beam lost some of its rf bunching in passing thru the lip on the Be target. The loss in duty factor due to rf bunching was only about a factor of 2. It was necessary to use four extraction targets of different lengths to cover the range from 5.0 GeV/c to 13.4 GeV/c.[26] The energy of the circulating beam was set slightly higher than the desired extracted beam energy to compensate for the energy loss in the extraction target. The absolute energy calibration was correct to $\pm\frac{1}{2}$% and the momentum spread of the beam was about ±5 MeV/c.

The extracted proton beam was transported from the ZGS to the CH_2 target by a system consisting of two quadrupole doublets with a bending magnet between them. The beam was collimated so that at the CH_2 target the angular divergence was $<\pm3$ mrad horizontally and $<\pm1$ mrad vertically at all energies. This gave a flux of $1\rightarrow 2\times10^{11}$ protons per pulse through the one-square-inch CH_2 target.

The beam was tuned by varying the current of the proton beam bending magnet. A triple scintillation counter telescope $B=B_1B_2B_3$ viewed a $\frac{1}{16}$-in.-thick Lucite flip target which was placed near the exit port of the ZGS. This target was upstream of all of the beam transport elements. A second monitor telescope $M=M_1M_2M_3$ viewed the CH_2 target. The ratio of M/B was maximized by varying the currents in the beam-bending magnet and thus sweeping the beam across the target. A typical beam magnet curve is shown in Fig. 2. Since the beam was not fully focused at the CH_2 target

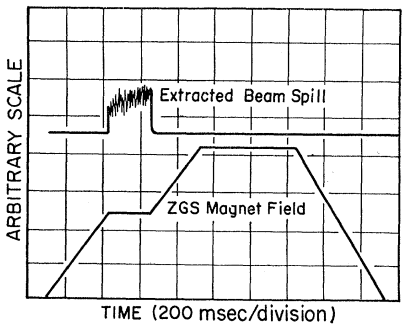

FIG. 1. Plot of ZGS magnetic field and beam spill during "front porch."

[20] G. Cocconi, V. T. Cocconi, A. D. Krisch, J. Orear, R. Rubinstein, D. B. Scarl, W. F. Baker, E. W. Jenkins, and A. L. Read, B. T. Ulrich; Phys. Rev. Letters **11**, 499 (1963); W. F. Baker *et al.*, *ibid.* **12**, 132 (1964); G. Cocconi *et al.*, *ibid.* **138**, B165 (1965).

[21] A. N. Diddens, E. Lillethun, G. Manning, A. E. Taylor, T. G. Walker, and A. M. Wetherell, *1962 International Conference on Higy Energy Physics* at CERN (CERN Scientific Information Service, Geneva, Switzerland), p. 576.

[22] A. R. Clyde, B. Cork, D. Keefe, L. T. Kerth, W. M. Layson, and W. A. Wenzel; *International Conference on High Energy Physics, Dubna 1964* (Atomizdat, Moscow, 1964); A. R. Clyde, thesis, UCRL-16275, 1966 (unpublished).

[23] J. V. Allaby, G. Bellettini, G. Cocconi, M. L. Good, A. N. Diddens, G. Matthlae, E. S. Sacharidis, A. Silverman, and A. M. Wetherall, Phys. Letters **23**, 389 (1966).

[24] B. Cork, W. A. Wenzel, and C. W. Causey, Phys. Rev. **107**, 859 (1957).

[25] G. Bellettini, G. Cocconi, A. N. Diddens, E. Lillethun, J. Pahl, J. P. Scanlon, J. Walthers, A. M. Wetherell, P. Zanella, Phys. Letters **14**, 164 (1965); see Bellettini *et al.* for other references.

[26] L. G. Ratner, Argonne National Laboratory-PAD Report No. LGR-7 (unpublished).

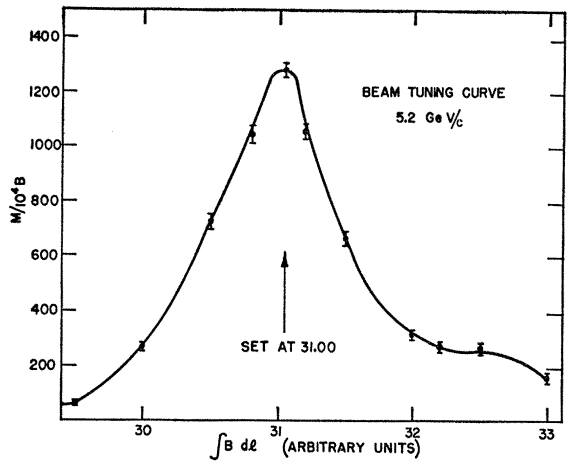

FIG. 2. Beam tuning curve showing the ratio of M monitor counts to B monitor counts as a function of current in the beam bending magnet.

it was not entirely possible to tune the quadrupoles by this method. These quadrupoles were set to values determined from computer programs. They were then checked by producing a focus at the CH_2 target by varying the quadrupoles in the appropriate way.

B. CH_2 Target and Monitoring

The target protons for the p-p scattering were provided by the hydrogen nuclei in the CH_2 target. The density of hydrogen in this target material was measured to be 0.131 g/cm^3. The targets used were 1 cm thick from 5.0 to 8.8 GeV/c and 2 cm thick from 9.0 to 13.4 GeV/c. A different target was used for each energy. In addition, carbon targets were used to determine the background due to quasielastic p-p scattering from the carbon nuclei in CH_2. As discussed in Sec. E, these quasielastic events comprised less than 1% of the total events at all energies.

The number of protons passing thru each target was determined by measuring the induced radioactivity in the target. When protons passed through the CH_2 target a Be^{7*} isotope was created in the spallation process.

$$p+C^{12}\rightarrow Be^{7*}+X. \quad (1)$$

The Be^{7*} nucleus decayed, with a mean life of 77.5 days, by K capture followed by the emission of a 0.48 MeV γ ray. This γ activity was measured in a standard γ spectrometer, which consisted of a NaI counting chamber, with a window bracketing 0.48 MeV. Background runs and subtractions were made with no CH_2 target in the counting chamber. This background was usually less than 1% because of the thick lead walls surrounding the counting chamber.

The absolute calibration[27] of the number of protons corresponding to a given number of Be^{7*} decays was obtained from calibration runs at 5, 7, 9, and 11 GeV/c. These runs were made with thin Au and Al foils taped on both the upstream and downstream ends of the CH_2 targets. These foils were carefully cut to ensure that the same number of protons passed thru both foils and the CH_2 target. The number of protons passing thru was then determined by measuring the production of F^{18}, Na^{24}, and Tb^{149} in each foil. These production cross sections are fairly well known. The Be^{7*} decay rate was also measured for each CH_2 calibration target. We thus obtained the ratio of Be^{7*} γ counts per minute to proton flux at the calibration momenta. We then could easily convert the number of gamma counts per minute into protons for each CH_2 target used in a data run.

The calibration runs were all consistent to within 2%. However, there is an over-all uncertainty in the F^{18}, Na^{24}, and Tb^{149} cross sections of about 5%. This introduced a possible normalization uncertainty, but no point-to-point systematic error. We obtained statistics of 1% or better on the counting of all CH_2 targets. We also had at least one rerun on each CH_2 target a week or two later. All reruns were consistent within statistics. Thus the proton flux thru each CH_2 target was known with a 2% relative error and a 5% normalization uncertainty.

One further comment is necessary about the monitoring of the incident proton flux. It was desirable to split each cross-section measurement into 5 to 10 runs. Since recording data took about a minute, the detection system for events was not switched on 100% of the time that protons were passing thru the CH_2 target. To take this into account a monitor telescope of scintillation counters $M=M_1M_2M_3$ looked at the CH_2 target as shown in Fig. 3. This was connected to two coincidence circuits as shown in Fig. 5: M, which was gated on and off along with the event detection system, and UGM which was ungated and thus turned on all of the time. Then the number of protons passing through the CH_2 target while the event detectors were gated on was given by

$$\text{protons}=\frac{M}{\text{UGM}}(\text{protons})_{\text{total}}. \quad (2)$$

For all data runs the ratio M/UGM was between 0.96 and 0.99, so that any systematic errors arising from dead times and accidentals were well below 1%.

C. Detection of Events

The two scattered protons were detected with the double spectrometer arrangement shown in Fig. 3. Each spectrometer basically consisted of a bending magnet for momentum analysis and a telescope of three scintillation counters to detect the particles.

The protons which were scattered through 90° in the center-of-mass system emerged at equal angles in the laboratory. They first passed through a C magnet

[27] J. B. Cumming, J. Hudis, A. M. Poskanzer, S. Kaufman, Phys. Rev. 128, 2392 (1962); J. B. Cumming, Ann. Rev. Nucl. Sci. 13, 261 (1963).

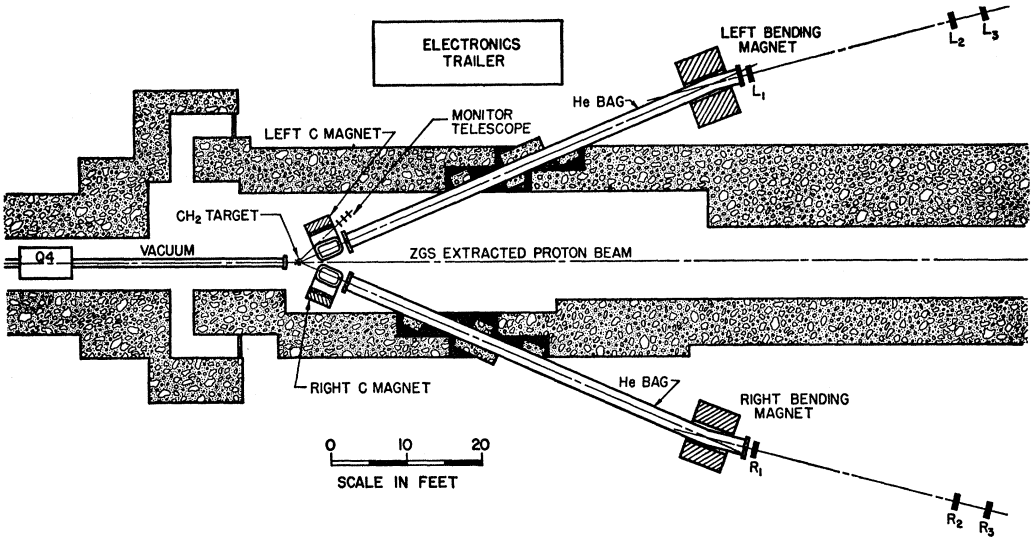

FIG. 3. Experimental layout; the incident protons come down the extracted beam and strike the target. The scattered protons pass out through the magnets and scintillation counters.

and then went out through the beam ports in the shielding. The protons were momentum-analyzed by a 9° deflection in the 72-in. bending magnet (B magnet) and then detected by a telescope of three scintillation counters ($L=L_1L_2L_3$ or $R=R_1R_2R_3$).

The center-or-mass solid angle was defined by the L_3 counter which was 7 in. × 5 in. and about 100 feet from the CH_2 target. To calculate this solid angle it was necessary to consider the dipole focusing due to the two magnets, by using standard magnet matrices. The laboratory solid angle varied between 4.32 and $2.96\ 10^{-5}$ sr because of this effect. The corresponding center-of-mass solid angle varied between 2.08 and $2.73\ 10^{-4}$ sr. The momentum bite defined by the left spectrometer was about ±10% while the momentum bite defined by the right spectrometer was about ±15%.

Because of the symmetry of the system at 90° the matched size of the R_3 counter was also 7 in. × 5 in. However, this counter was overmatched to insure that "in-scattering" was equal to "out-scattering" so that no correction to the raw data was necessary. In a coincidence experiment one must be sure that when a proton scattered into the L_3 counter its mate proton also went thru the R_3 counter. Thus the R_3 counter was chosen to be 12 in. × 10 in. in size. This gave a 2.5 in. strip around the matched size which allowed for out-scattering due to the following experimental difficulties: angular divergence of the incident beam, ±3 mrad horizontally, ±1 mrad vertically; momentum spread of the incident beam, ±1%; multiple scattering in the CH_2 target, the air, the He bags, and the early scintillators; a 1% error in the $\int \mathbf{B}.d\mathbf{l}$ of any of the four analyzing magnets; and the 1 in. × 1 in. target spot size. All other counters were also overmatched; thus L_3 alone defined the solid angle of the detection spectrometers.

The C magnets solved a problem caused by the energy dependence of the Lorentz transformation from the center-of-mass system to the laboratory system. This made the 5.0 GeV/c protons come out at 29.16° while the 13.4 GeV/c protons came out at 19.87°. Without the C magnets, it would have been necessary to move the bending magnets more than 10 feet in 50 separate steps during the course of the experiment. However, the system was designed so that at 9.4 GeV/c, where the protons were scattered at 23.03°, the C magnets were turned off. At 5.0 GeV/c, the 29.16° protons were bent in by 6.13°, while at 13.4 GeV/c the C magnets were reversed and the 19.87° protons were bent out by 3.16°. Thus the protons always emerged from the C magnets at 23.03°. The 5.0 and 13.4 GeV/c scattered protons emerged only 8 in. apart and easily fit throu the 24-in. aperture of the bending magnets. The bending magnets were adjusted so that the protons always passed through the centers of the L_3 and R_3 counters.

This technique had two important advantages. First, it eliminated costly moves of heavy magnets. Second, it eliminated possible systematic errors due to misalignment of magnets and counters in going from one energy to another. Changing energies involved only varying the magnet currents. The scintillation counters were not moved. No timing change was necessary between the L and R telescopes because the spectrometers were of equal length and the two protons had equal velocities. Thus, there was essentially no point-to-point systematic error due to losses in the detection spectrometers.

The C magnets had pole faces 15 in. wide by 30 in.

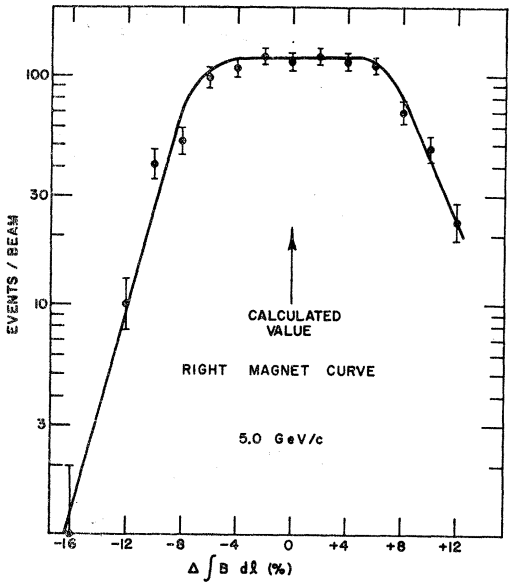

FIG. 4. Right bending magnet curve showing the number of left-right coincidences as a function of magnet current. This gave a check of the amount of counter overmatching.

long with a 10-in. gap width. The bending magnets were of the standard "picture-frame" type; each was 72 in. long and the left one had a 6 in. × 30 in. gap while the right one had an 8 × 24 in. gap. The magnetic field integrals $\int \mathbf{B} \cdot d\mathbf{l}$ were calibrated using nuclear magnetic resonance and floating-wire techniques. These calibrations agreed well with previous measurements[28] by the ZGS staff. During the experiment the magnet currents were set by reading the voltage across a standard shunt with two digital voltmeters in parallel. In addition each C magnet was monitored continuously with NMR probes. All field integrals were known to $\pm\frac{1}{2}\%$.

The calibration and alignment of the spectrometers were tested by running a right magnet curve. This consisted of measuring the number of 90° proton-proton elastic scattering events at 5.0 GeV/c while varying the current in the right bending magnet. Everything else was held fixed. The resulting curve is shown in Fig. 4. First notice that the curve was centered about the calculated value. This showed that all magnets had correctly calibrated field integrals, and that all angles had been correctly surveyed. Next notice that there was a flat top about $\pm 5\%$ wide. This indicated that the horizontal overmatching on the R_3 counter was sufficient. If the overmatching had been insufficient there would have been no flat top. The overmatching was also checked by taking test runs with a smaller (4 in. × 4 in.) L_3 counter.

[28] R. J. Lari, Argonne National Laboratory-PAD Reports Nos. RJL-2, RJL-3, RJL-5, RJL-6 (unpublished).

D. Counters and Electronics

The L and R counter telescope each consisted of three Pilot B plastic scintillators. These were $\frac{1}{2}$ in. thick and rectangular, varying in size from 7 in. × 5 in. to 19 in. × 8 in. The scintillators were optically connected to RCA 7746 photomultiplier tubes by Lucite light pipes. These are fast 10 stage tubes which were operated at about 1800 V. The output signals from these tubes were carried to the electronic logic system by RG 8U, 50Ω, cables which were about 100 feet long. The high voltage on the tubes was supplied by 3 kV power supplies via a distribution panel and read on two Hewlet-Packard 3440A 4-place digital voltmeters in parallel.

The logic system consisted of 100 Mc Chronetic coincidence circuitry. A block diagram of the logic system is shown in Fig. 5. The signal cables used within the system were 50Ω, RG223. The output of the logic system was displayed on 100 Mc, TSI 1535 scalers and recorded with a Polaroid camera. The 400-channel pulse-height analyzer was a TMC model 404C. Important quantities were double scaled. The three L signals; L_1, L_2, and L_3 came together to form a three-fold L coincidence. Similarly, R_1, R_2, and R_3 formed an R coincidence. The resolving times were about 5 nsec. The L and R signals were fed into the LR_{fast} coincidence circuit. If they arrived simultaneously within the 5 nsec resolving time they formed an LR_{fast} coincidence. The number of LR_{fast} coincidences would be equal to the number of elastic scattering events if they were no accidental events.

Two techniques were used to estimate the number of

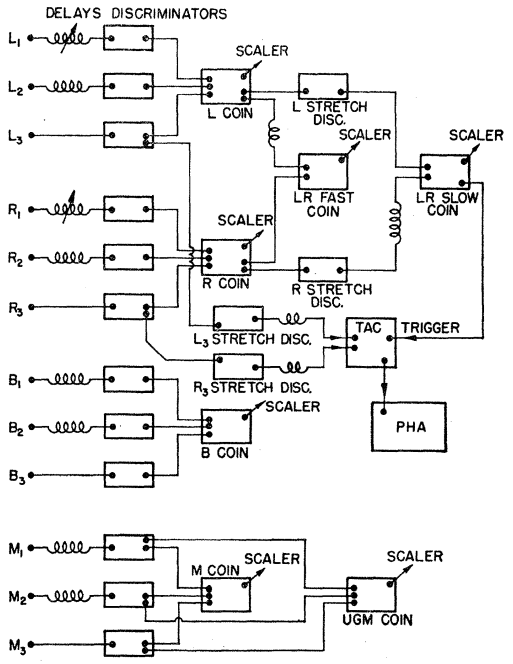

FIG. 5. Block diagram of circuitry for slow and fast coincidences and for pulse-height analysis.

accidentals. The first employed the LR_{slow} coincidence circuit, which had a 30 nsec resolving time, in contrast to the 5 nsec resolving time of the LR_{fast} coincidence circuit. If the number of LR_{slow} coincidences was equal to the number of LR_{fast} coincidences this was an indication that there were no accidentals and all coincidences were true events. If LR_{slow} was greater than LR_{fast} then the quantity $(LR_{\text{slow}}-LR_{\text{fast}})$ was some measure of the accidentals, assuming the two resolving times were well known.

The second, more reliable technique, used a time to amplitude converter (TAC) and a pulse-height analyzer (PHA). Each LR_{slow} pulse triggered the TAC. Stretched pulses from L_3 and R_3 were fed into the TAC which gave out a pulse whose height in volts was proportional to the time overlap of the L_3 and R_3 pulses. This was then fed into the PHA which sorted the pulses into bins according to pulse height and then stored and displayed the number of pulses in each bin. Thus the PHA gave a display of the number of events versus the time of flight difference between the left and right protons. Such a time of flight spectrum is shown in Fig. 6. Each channel is about 0.4 nsec wide. The true events appeared as a large peak about 1.6 nsec wide at half-maximum. The accidentals appeared as a broad flat region about 30 nsec wide, which could be subtracted from the peak. The subtraction varied from 0% at low energy to about 5% at 13.4 GeV/c. Because the broad region was so much wider than the peak the subtraction could be determined very accurately. The error due to this subtraction was always less than 1%.

The accidental rate was low because of the relatively low single telescope rates. The ratios of singles to elastic events varied between $L/LR=20\rightarrow 2000$ and $R/LR=100\rightarrow 20000$ in going from $5.0\rightarrow 13.4$ GeV/c.

E. Background

It was necessary to show that the system detected only proton-proton elastic scattering events. Two possible sources of background were quasielastic proton-proton scattering from the protons of the carbon nuclei in the CH_2, and inelastic proton-proton events in which one or more mesons were produced.

The quasielastic scattering was studied experimentally by taking runs with a pure carbon target substituted for the CH_2 target. At 5.0 GeV/c we took two equivalent runs with CH_2 and carbon targets; with CH_2 there were 1500 events, with carbon there was 1 event. At the highest energies we could not set such a low limit because there were some accidental events with both CH_2 and carbon targets. However it was possible to set a 1% upper limit at all energies. No carbon subtraction was made.

It was necessary to show that the detection system was not sensitive to inelastic proton-proton scattering events. The process most likely to mimic an elastic event was π^0 production.

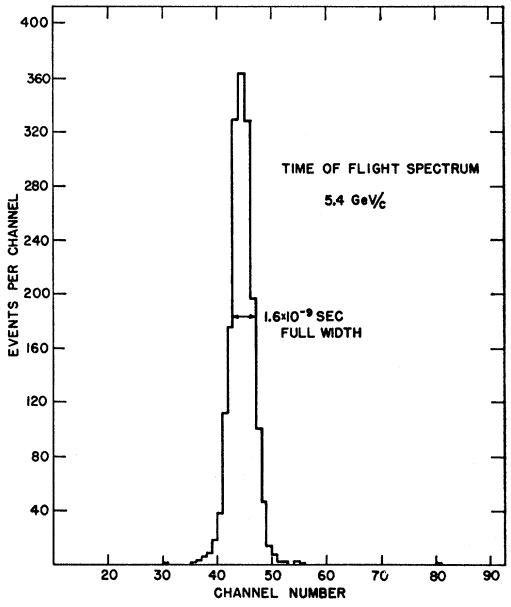

FIG. 6. Resolution curve from the pulse-height analyzer. Number of coincidences is plotted against the time-of-flight difference of left and right protons.

$$p+p\rightarrow p+p+\pi^0. \tag{3}$$

The carbon runs discussed above also serve as evidence that our system was not sensitive to events of this type.

To see this we first note that π^0 production smears proton-proton elastic kinematics more than the Fermi momentum of the protons in the carbon nucleus: the Fermi momentum is about 220 MeV/c corresponding to an energy of about 25 MeV, while the π^0 mass alone is 140 MeV, and no momentum-transfer distributions narrower than 100 MeV/c have ever been observed in this kind of process. Thus the π^0 production clearly smears things more than the Fermi momentum. Since the carbon runs show that the Fermi momentum was sufficient to knock quasielastic events out of our detection system, then the π^0 production surely knocked the protons out of our system. Thus from the carbon runs we set an upper limit of $\frac{1}{2}$% on inelastic production at all energies. No subtraction was made for inelastic events.

The reason for the small background lay in our tight kinematic constraints. The solid angle was 2×10^{-4} sr in the center of the mass and about 3×10^{-5} sr in the laboratory. The momentum bites of the two spectrometers were ±10% and ±15%. Moreover since we measured the angles and momenta of all particles we had a 4-constraint fit. These constraints strongly discriminated against any reaction other than proton-proton elastic scattering.

3. RESULTS

A. Corrections and Experimental Errors

The main correction to the raw data was for the possible loss of either of the two scattered protons due to nuclear interactions before reaching the final scintillation counter. Each proton had a 1% chance of interacting in the second half of the 1-cm CH_2 target and a 2% chance in the 2-cm target. There was a 2.4% chance of interacting in the air, a 0.5% chance of interacting in the He bag and windows, and a 2.5% probability of interacting in each of the first two scintillators. The only uncertainty comes from the fact that a nuclear interaction often gave a fast forward charged particle which may have triggered the last scintillation counter. The probability of this occurring was estimated for each different region. When this was taken into account, the total correction to the raw data was 1.14 for the 1-cm target and 1.16 for the 2-cm target. There was a $\pm 2\%$ uncertainty in these numbers which appeared only as a normalization uncertainty because the spectrometers were identical for all measurements.

There was a subtraction for accidental events discussed in Sec. 2D. This varied between 0 and 5%. The uncertainty in this correction was always less than 1%.

As discussed in Sec. 2E there was no correction for quasielastic or inelastic events. We set upper limits on these of 1% and $\frac{1}{2}$%.

Since the magnets and counters were not moved throughout the experiment there was no possibility of systematic errors due to misalignment of equipment. The only possible error was due to incorrect magnet currents. However there was sufficient overmatching to allow for a 1% error in any magnetic field integral. Since the estimated uncertainty in the field integrals was $\frac{1}{2}$% no correction was made.

The most significant source of systematic error came from the determination of the incident proton flux. As discussed in Sec. 2B there is some uncertainty in the cross sections for F^{18}, Na^{24}, and Tb^{149} production in Au and Al. This gave a 2% relative systematic error and a 5% normalization uncertainty.

The statistical uncertainty in the number of events varied between 2.1 and 6.8%. The relative systematic error of 2% was added in quadrature to this so that the total relative error varied between 2.9 and 7.1%.

In addition to this there was a normalization uncertainty which may shift all points up or down by about 7%. The incident proton momentum was known to about $\frac{1}{2}$%.

B. Calculation of Cross Section

The differential cross section was calculated from the formula

$$\frac{d\sigma}{d\Omega}=\frac{\text{events}}{I_0\Delta\Omega N_0\rho t}. \tag{4}$$

Here I_0 is the incident proton beam flux as measured by Be^{7*} decays, and $\Delta\Omega$ is the center-of-mass solid angle which was around 2×10^{-4} sr. The quantity N_0 is Avogadro's number taken to be $6.02\ 10^{23}$; t is the target thickness, either 1 or 2 cm; and ρ is the density of hydrogen protons in our block of CH_2 which was measured to be 0.131 moles/cm^3. The number of events was corrected as discussed above.

The resulting cross sections are tabulated in Table I for the 51 points with P_0 between 5.0 and 13.4 GeV/c. In addition to $d\sigma/d\Omega$, we have listed $d\sigma/dt$, P_0, $P_{c.m.}^2$ and the total error of each measurement. The results are also plotted in Fig. 7 where the cross section is seen to drop by almost four decades.

TABLE I. Proton-proton elastic scattering cross sections at 90° in the center-of-mass system.

$P_{c.m.}^2$ (GeV/c)^2	P_0 (GeV/c)	$(d\sigma/d\Omega)_{c.m.}$ (μb/sr)	$(d\sigma/dt)_{c.m.}$ μb/(GeV/c)^2	Error in $d\sigma/d\Omega$ & $d\sigma/dt$ %
1.946	5.0	8.51	13.74	2.9
1.993	5.1	7.90	12.45	3.3
2.039	5.2	7.09	10.93	3.1
2.086	5.3	6.49	9.77	3.6
2.132	5.4	5.53	8.15	3.1
2.178	5.5	4.90	7.07	3.4
2.223	5.6	4.47	6.32	3.1
2.270	5.7	3.72	5.15	3.3
2.316	5.8	3.37	4.57	3.3
2.363	5.9	2.74	3.64	3.5
2.409	6.0	2.44	3.18	3.1
2.456	6.1	2.19	2.80	3.7
2.503	6.2	1.83	2.30	3.7
2.595	6.4	1.50	1.82	3.7
2.686	6.6	1.07	1.25	4.7
2.779	6.8	0.796	0.900	4.7
2.873	7.0	0.645	0.706	4.1
2.965	7.2	0.515	0.546	4.0
3.059	7.4	0.386	0.396	4.8
3.151	7.6	0.305	0.304	5.4
3.247	7.8	0.253	0.245	4.5
3.338	8.0	0.217	0.204	4.5
3.386	8.1	0.169	0.157	3.9
3.434	8.2	0.172	0.157	4.4
3.480	8.3	0.154	0.139	3.8
3.527	8.4	0.153	0.136	4.6
3.618	8.6	0.127	0.110	4.6
3.713	8.8	0.103	0.0871	4.8
3.806	9.0	0.0809	0.0667	4.6
3.897	9.2	0.0780	0.0629	4.3
3.992	9.4	0.0676	0.0532	5.3
4.084	9.6	0.0589	0.0453	4.9
4.178	9.8	0.0536	0.0403	4.7
4.272	10.0	0.0468	0.0344	4.9
4.364	10.2	0.0441	0.0318	4.8
4.461	10.4	0.0386	0.0272	4.7
4.554	10.6	0.0356	0.0246	4.8
4.644	10.8	0.0303	0.0205	4.9
4.739	11.0	0.0284	0.0188	5.5
4.831	11.2	0.0255	0.0166	5.4
4.924	11.4	0.0202	0.0129	5.4
5.018	11.6	0.0190	0.0119	5.2
5.112	11.8	0.0153	0.00940	5.4
5.208	12.0	0.0143	0.00862	5.4
5.299	12.2	0.0118	0.00699	5.3
5.392	12.4	0.0116	0.00676	5.4
5.490	12.6	0.00953	0.00545	6.3
5.579	12.8	0.00867	0.00488	5.7
5.674	13.0	0.00739	0.00409	5.9
5.770	13.2	0.00722	0.00393	7.1
5.861	13.4	0.00525	0.00281	5.7

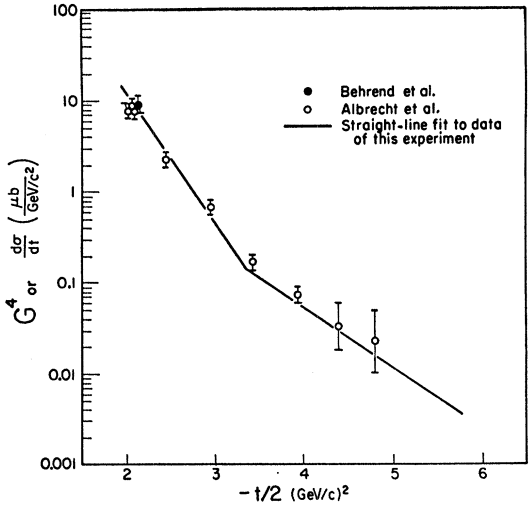

FIG. 7. Plot of $d\sigma/dt$ versus $P_{c.m.}^2$ for proton-proton elastic scattering at 90° in the center-of-mass system. Other data (Refs. 20, 22, 23) are also plotted. The lines drawn are straight line fits to the data.

4. DISCUSSION OF RESULTS

In the past few years there has been considerable speculation about the meaning and significance of the behavior of the elastic scattering cross section of strongly interacting particles. There has been interest in both the small and large momentum transfer regions, in addition to very recent interest in backward scattering which we shall not discuss. Models explaining some aspects of the data had come to be more or less accepted, while other aspects of the data continued to be equally well interpreted by many different models. There was a clear need for new measurements with smaller errors to distinguish between these various models.

The behavior of small-angle elastic scattering is probably understood phenomenologically. It is dominated by the diffraction scattering associated with the many inelastic processes that become very important at high energies. Diffraction models have been suggested and studied by many authors.[29–33]. The main evidence for the dominance of the diffraction mechanism lies in the fact that the forward-scattering amplitude is mainly imaginary at high energy. Recent experiments[2,34] indicate that the real part of the forward amplitude is 20% or less at high energies. Other evidence, which has recently been noted[32,35] is that the slope of the diffraction peak (A in $d\sigma/dt \propto e^{-At}$) in $\pi p, kp$, and p-p scattering is roughly proportional to the corresponding inelastic cross sections. This is consistent with the diffraction concept that $\sigma_{in}=\pi R^2$ and $A=\frac{1}{2}R^2$. There may still be some confusion about the shrinking and nonshrinking of various diffraction peaks. But this confusion seems to arise primarily from uncertainty about which variable $d\sigma/dt$ should be plotted against in a correct diffraction model.

In the large momentum-transfer region there has been much more uncertainty. Some authors[29–33] suggested that the diffraction scattering still dominated here. Another group[36] advocated a type of statistical model. In addition, a wide range of other models[35,37,38] and ideas were suggested. The experiment[20] which either stimulated or tested most of these ideas measured the differential proton-proton cross section over almost seven decades, but the errors in these measurements were too large to allow discrimination against many of the models.

There were several features of the present experiment[39] which allowed it to distinguish between the predictions of different models. First, it contained 51 closely spaced measurements in the range 5.0 to 13.4 GeV/c where the cross section decreased by about four decades. Moreover, the errors were quite small; almost all errors were between 3 and 6%. These small errors together with the close spacing of the data points allowed one to easily distinguish between different fits to the data. Finally, this experiment eliminated confusion about the choice of the correct variable. Since all cross sections were measured at 90° where $\sin\theta=1$ and $\cos\theta=0$; we have that $P_{c.m.}^2=P_\perp^2=-t/2$. Thus, both variables were proportional to each other and there was no confusion.

A. Dibaryon Resonances

A useful technique of finding resonances and studying their properties consists of measuring the energy dependence of a differential cross section at a fixed angle.

[29] R. Serber, Phys. Rev. Letters **10**, 357 (1963); R. Serber, Rev. Mod. Phys. **36**, 649 (1964).
[30] A. D. Krisch, Phys. Rev. Letters **11**, 217 (1963).
[31] A. D. Krisch, Phys. Rev. **135**, B1456 (1964).
[32] A. D. Krisch, *Lectures in Theoretical Physics* (University of Colorado Press, Boulder Colorado (1966), Vol. IX.
[33] H. H. Aly, D. Lurie, and S. Rosendorff, Phys. Letters **7**, 198 (1963); S. Minami, Phys. Rev. Letters **12**, 200 (1964); Phys. Rev. **135**, B1263 (1964); H. A. Bethe, Nuovo Cimento **33**, 1167 (1964); A. Baiquni, Phys. Rev. **137**, B1009 (1965); W. N. Cottingham and R. F. Peierls, *ibid.*, **137**, B147 (1965); E. M. Henley aud I. J. Muzinich, *ibid.* **136**, B1783 (1964); M. L. Perl, M. C. Corey, *ibid.* **136**, B787 (1964); L. M. Simmons, Phys. Rev. Letters **12**, 229 (1964); T. T. Wu and C. N. Yang, Phys. Rev. **137**, B708 (1965); K. Huang, *ibid.* **146**, 1075 (1966); L. Van Hove, Nuovo Cimento **28**, 798 (1963); Phys. Letters **5**, 252 (1963); **7**, 76 (1963); Rev. Mod. Phys. **36**, 655 (1964).
[34] G. Bellettini, G. Cocconi, A. N. Diddens, E. Lillethun, J. Pahl, J. P. Scanlon, J. Walthers, A. M. Wetherell, and P. Zanella, Phys. Letters **14**, 164 (1965).
[35] C. H. Woo, Phys. Rev. **150**, 1372 (1966).
[36] G. Fast and R. Hagedorn, Nuovo Cimento **27**, 203 (1963); G. Fast, R. Hagedorn, and L. W. Jones, *ibid.* **27**, 856 (1963); G. Cocconi, *ibid.* **33**, 643 (1964); L. W. Jones, Phys. Letters **8**, 287 (1964); R. Hagedorn, Nuovo Cimento **35**, 210 (1965); G. Auberson and B. Escoubes, Nuovo Cimento (to be published); A. Bialas and V. Weisskopf, Nuovo Cimento **35**, 1211 (1965); J. Vandermeulen, University of Liege, Belgium, 1964 (unpublished); H. Joos and H. Satz, Nuovo Cimento **34**, 619 (1964).
[37] K. Yamamoto, Phys. Rev. **134**, B682 (1964), and Enrico Fermi Institute for Nuclear Studies Report 64-11 (unpublished); A. P. Balachandran, Phys. Rev. **137**, B177 (1965); J. Orear, Phys. Letters **13**, 190 (1964); M. N. Focacci and G. Giacomelli, CERN Report No. 66-18; M. M. Islam (unpublished).
[38] D. S. Narayan and K. V. L. Sarma, Phys. Letters **6**, 365 (1963).
[39] C. W. Akerlof, R. H. Hieber, A. D. Krisch, K. W. Edwards, L. G. Ratner, K. Ruddick, Phys. Rev. Letters **17**, 1105 (1966).

This technique has been used often in nuclear physics and has recently been used[12,40] to study N^* resonances in high-energy $\pi^- p$ elastic scattering at 180°. In the present experiment, a dibaryon resonance would have shown itself as an intermediate state in the process

$$p+p \rightarrow B^2 \rightarrow p+p. \quad (5)$$

The amplitude for this process would then interfere with the amplitude for the rest of the elastic scattering. It could interfere either constructively, destructively, or not at all. The existence of this mechanism for producing structure in a fixed-angle cross section was demonstrated in the recent 180° $\pi^- p$ elastic-scattering experiment. However, in the present cross section there are clearly no bumps or valleys, as can be seen in Fig. 7. In fact, we can set an upper limit on any fluctuations, at a level which goes from 5% at 5.0 GeV/c to 10% at 13.4 GeV/c. Now, ignoring the possibility of spin-flip amplitudes, the resonant amplitude for even-l states is given by

$$f_l^R(90°)=\frac{i\hbar}{P_{\text{c.m.}}}(2l+1)P_l(90°)\chi_l(e^{2i\delta_l}-1). \quad (6)$$

The quantity $(2l+1)P_l(90°)$ is equal to 1 for $l=0$ and is larger for all higher values of l. Let us now assume that there is a dibaryon resonance so that $\delta_l=90°$ and

$$e^{2i\delta_l}-1=-2. \quad (7)$$

Then we have an upper limit on the elasticity of any such resonance with even l, $S=0$ and $T=1$.

$$\begin{aligned}\chi_l &< 0.005 \text{ at } 5.0 \text{ GeV}/c \\ &< 0.0005 \text{ at } 13.4 \text{ GeV}/c.\end{aligned} \quad (8)$$

If we include spin-flip terms in the resonant amplitude, then we will get mixing between odd and even l states in Eq. (6). This will yield a similar upper limit on the elasticity of odd l, $S=0$, $T=1$ dibaryon resonances.

B. Statistical Model

Next we consider the type of statistical model which has recently been advocated by Hagedorn and others.[36] The basic idea is that two high-energy particles can stick together and form an excited state which subsequently decays into any of the allowed channels, including the elastic channel. It is assumed that all channels have roughly equal probabilities and the elastic channel has an approximately isotropic angular distribution.

There now seems to be some evidence that this type of statistical mechanism does not dominate the high momentum-transfer region. A recent CERN experiment[23] found no Ericson fluctuations[41] in a fixed-energy angular distribution, and we find no Ericson fluctuations in a fixed-angle energy distribution. One of the necessary assumptions of the statistical model is the existence of an intermediate excited state which can decay into many different channels. As pointed out in the previous section, we find no evidence for the existence of any discrete resonances as excited intermediate states in the proton-proton system. If there are no Ericson fluctuations, this implies that there are no overlapping intermediate states. If indeed no such excited states exist, a statistical model is hard to justify.

Finally we note that the statistical model of Hagadorn and others predicted that the differential cross section at 90° behaves according to

$$d\sigma/d\Omega=Ae^{-P_{\text{c.m.}}/P_0}. \quad (9)$$

Here P_0 is a constant taken to be about 155 MeV/c. This prediction was not in disagreement with the Cornell-BNL data.[20] However when the present, small-error, data are plotted against $P_{\text{c.m.}}$ as in Fig. 8, the disagreement is evident. The data appear S-shaped with at least 25 points missing a straight line by 10 or more standard deviations. We regard this as further evidence that the statistical model is not useful in the range 5.0 to 13.4 GeV/c. We can make no statement about the validity of the statistical model at higher energies.

C. Analyticity of the Scattering Amplitude

In the past few years Cerulus and Martin, and Kinoshita[42] have studied the limits which can be set on scattering amplitudes with only very general assump-

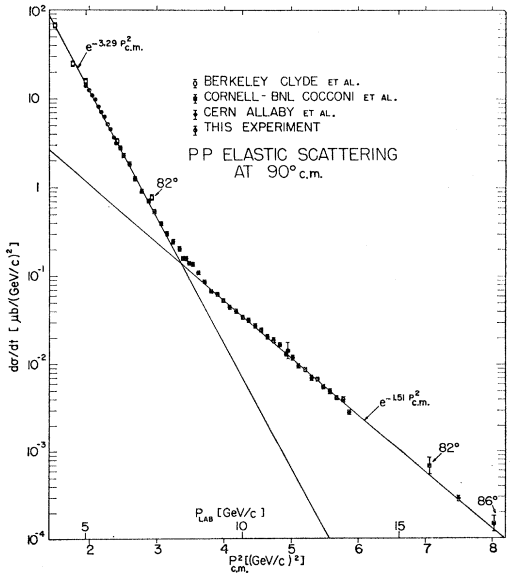

FIG. 8. Plot of $d\sigma/d\Omega$ versus $P_{\text{c.m.}}$ for 90° proton-proton elastic scattering. Other data (Refs. 20, 22, 23) are also plotted. The line drawn is the straight line fit suggested by the statistical model.

[40] R. Heinz and M. Ross, Phys. Rev. Letters 14, 1091 (1965); B. Jacobsohn and C. N. Yang (private communication); V. Barger and D. Cline, Phys. Rev. Letters 16, 913 (1966).

[41] T. Ericson, CERN Report No. TH406 (1964) (unpublished); Ann. Phys. (N. Y.) 23, 390 (1963); T. Ericson and T. Mayer-Kuckuk, CERN Report No. 66/TH686 (unpublished).

[42] F. Cerulus and A. Martin, Phys. Letters 8, 80 (1964); T. Kinoshita, Phys. Rev. Letters 12, 257 (1964).

TABLE II. The slopes and corresponding radii of the three regions.

	Slope in $P_{c.m.}^2$ plot	Radius from $P_{c.m.}^2$ plot	Slope in $\beta^2 P_\perp^2$ plot	Radius from $\beta^2 P_\perp^2$ plot
	A in $\exp(-AP_{c.m.}^2)$ $(\mathrm{GeV}/c)^{-2}$	$R=\hbar c\sqrt{(2A)}$ (F)	B in $\exp(-B\beta^2 P_\perp^2)$ $(\mathrm{GeV}/c)^{-2}$	$R=\hbar c\sqrt{(2B)}$ (F)
Outer	...	...	$10 \rightarrow 11$	$0.88 \rightarrow 0.92$
Intermediate	3.29	0.51	3.48	0.52
Inner	1.51	0.34	1.52	0.34

tions. In fact, they showed that if the scattering amplitude is analytic and bounded then the fixed angle differential cross section cannot decrease as fast as e^{-s}, in the asymptotic region $s \rightarrow \infty$. In Fig. 7 one can see that the data are well fitted by

$$d\sigma/dt = Ae^{-1.52P_{c.m.}^2}. \tag{10}$$

Since for proton-proton scattering it is true that

$$s = 4P_{c.m.}^2 + 4m^2, \tag{11}$$

we can rewrite Eq. (10) as

$$d\sigma/dt = (Ae^{+1.52m^2})e^{-.38s}. \tag{12}$$

If the cross section continues to fall this rapidly in the asymptotic region, the lower bound will be violated.

However it should be pointed out that the cross section can fall as rapidly as

$$\frac{d\sigma}{dt} = \frac{Be^{-c\sqrt{s}}}{P(s)}, \tag{13}$$

where $P(s)$ is any finite polynomial in s, without violating the lower bound. It is unlikely that experiments will be able to distinguish between e^{-As} and Eq. (13) where $P(s)$ is a high-order polynomial.

D. Structure within the Proton

Perhaps the most striking feature of our data is the sharp break in the cross section which can be seen in Fig. 7. We believe that such a sharp change can only be interpreted as evidence for the existence of more than one type of process. In fact, we believe that the several regions seen in the scattering cross section are firm evidence for the existence of several regions within the proton.

In Fig. 7 we plotted the differential cross section at 90° as a function of $P_{c.m.}^2$. Since at 90° $P_{c.m.}^2 = P_\perp^2 = -t/2$, we really have a conventional plot of $d\sigma/dt$ against transverse momentum-squared or momentum transfer. Nevertheless, it is desirable to show that the data away from 90° exhibits the same sort of behavior. To demonstrate this we must return to the problem of choosing a "correct" variable which removes the energy dependence or "shrinkage." It has been suggested by one of the authors[32] that $d\sigma/dt$ should be plotted against $\beta^2 P_\perp^2$. The cross section would depend only on this variable in a diffraction model with a spherically symmetric interaction probability density $P(R)$ which is Lorentz contracted in the direction of the incident motion. Notice that

$$\beta^2 P_\perp^2 = (1-1/\gamma^2)P_\perp^2 \xrightarrow[\lim \gamma \rightarrow \infty]{} P_\perp^2. \tag{14}$$

Thus at infinite energy, a sphere gets squashed down to a disk, so that the interaction probability density depends only on the impact parameter $R_\perp$. Then the cross section will depend only on the canonically conjugate variable $P_\perp$.[30,38] At finite energies the factor $1/\gamma^2$ comes in because the sphere is only squashed down by a factor $1/\gamma$.

Thus in Fig. 9 we plot $d\sigma/dt$ against $\beta^2 P_\perp^2$ for high energy proton-proton elastic scattering data of all angles. One can clearly see the three regions in the cross-section plot; the two regions seen in our 90° data, in addition to the small angle diffraction peak. The slopes of these three regions are well determined from Fig. 9 and also Fig. 7. These are tabulated in Table II along with the corresponding radii. These radii are determined by looking at the Fourier transform of the

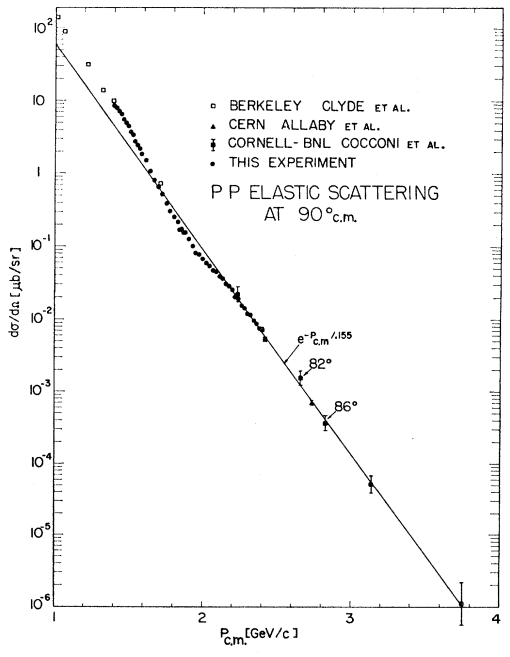

FIG. 9. Plot of $d\sigma/dt$ versus $\beta^2 P_\perp^2$ for all high-energy proton-proton elastic scattering. Other data (Refs. 13, 20, 22, 23), are also plotted. The lines drawn are straight line fits to the data.

Gaussian interaction probability density

$$P(R)=e^{-\frac{1}{2}R^2/A^2}. \tag{15}$$

Taking the Fourier transform of this distribution gives a 90° differential cross section of the form

$$\frac{d\sigma}{dt}=\left(\frac{d\sigma}{dt}\right)_0 e^{-\frac{1}{2}P_{\text{c.m.}}{}^2A^2}. \tag{16}$$

Thus there appear to be three distinct regions in the cross section. This has two possible interpretations in terms of structure in the proton; the "proton" can either have two or three regions. This ambiguity arises from the fact that our experiment does not study what one proton looks like, but rather what one proton looks like to another proton. Thus any spatial distribution that might be implied by this experiment is really the interaction probability density as a function of the distance between the protons. There is some uncertainty about how one obtains information about a single proton from this distribution.

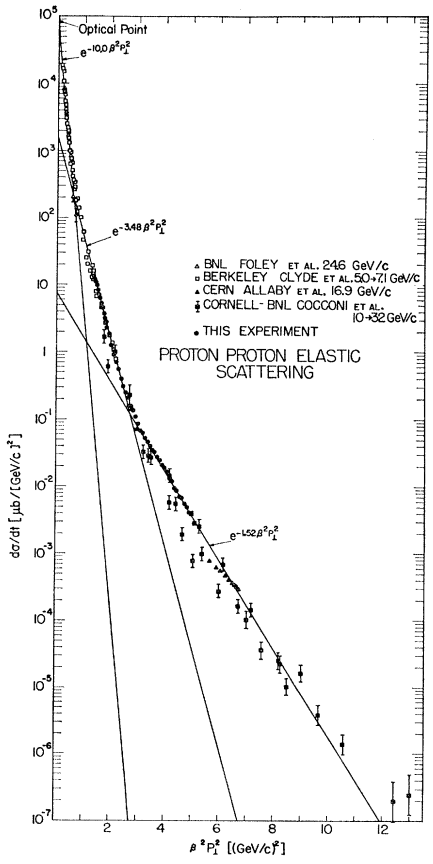

FIG. 10. Plot of $d\sigma/dt$ versus $P_{\text{c.m.}}{}^2$ for proton-proton elastic scattering at 90°, comparing it to electron-proton elastic scattering at high momentum-transfer. The lines drawn are the straight line fits to the proton-proton data. The electron-proton data (Ref. 44) are plotted as the fourth power of the form factor, and are normalized to the proton-proton cross section.

One possible explanation is that the interaction probability density we observed, with its three regions, is some kind of convolution of the two protons. Then to obtain a picture of a single proton one must take some sort of square root. To illustrate this idea we consider the example of a proton which consists of a core surrounded by a cloud. Then when two of these protons interact there will be three types of interactions: cloud-cloud, cloud-core, and core-core. Thus there would appear to be three regions as we observe. Unfortunately, to take this seriously one needs a model for how the two protons are folded together. This model would give a relationship between the three observed radii in terms of the cloud and core radii. The simple ideas for folding the protons together do not seem to agree with the observed radii, but perhaps someone can devise a sensible model of this type that works.

Another possible interpretation of our data is somewhat more phenomenological. It suggests that it may be most useful to consider the interaction probability density of two interacting protons, without any great concern for what one proton looks like. One might then speculate on what other properties of the proton-proton interaction might be deduced from the three regions seen in elastic scattering. One model[31,32] of this type suggests that the three regions may be the diffraction scattering associated with three different types of inelastic processes.

Finally it is interesting to try to compare our data with electron-proton scattering data. It should be pointed out that electron-proton data has not shown evidence for the sharp break that we observe. However, we believe that the electron-proton data is not inconsistent with this break.

In order to compare electron-proton and proton-proton data one needs some model to express one of these results in terms of the other. One such device is the recent speculation by Wu and Yang[43] that

$$\frac{d\sigma}{dt}(pp)\propto[G(ep)]^4. \tag{17}$$

Here $G(ep)$ is the electromagnetic form factor of the proton, which is extracted from the electron-proton scattering data. Using this idea we have prepared Fig. 10 in which we plotted the high-momentum transfer form factors[44] along with the straight line fits to our 90° proton-proton data. As one can see they are not at all inconsistent. However it should be noted that the corresponding electron-proton errors are considerably larger than ours. The errors in the form factors are already larger than ours and these must be multiplied by a factor of four because the form factor is taken to the fourth power. Thus one cannot claim that the

[43] T. T. Wu and C. N. Yang, Phys. Rev. **137**, B708 (1965).

[44] W. Albrecht, H. J. Behrend, F. W. Brasse, W. Flauger, H. Hultschig, and K. G. Steffen, Phys. Rev. Letters **17**, 1192 (1966). See this paper for earlier references.

electron-proton data contain any conclusive evidence for the several regions we see.

Finally, we point out that the break in the proton-proton cross section seen in Fig. 7 is indeed very sharp. At the point where the two exponentials cross, the data are only about 25% above the intercept. Two exponentials adding completely incoherently would give a cross section a factor of 2 above the intercept, while two amplitudes interfering constructively would result in a curve which was a factor of 4 above the intercept. The factor 1.25 appears to indicate partial destructive interference between the two amplitudes. We do not understand the significance of this.

ACKNOWLEDGMENTS

We would like to thank the entire ZGS staff for their help and encouragement during the experiment, and Dr. E. Steinberg and Dr. A. Stehney for their aid and advice in the radiochemical analysis of the targets. We also thank Professor M. H. Ross, Professor G. L. Kane, and Professor E. Loman for their helpful comments.

PHYSICAL REVIEW VOLUME 159, NUMBER 5 25 JULY 1967

Low-Energy (Σ^+,p) and (Σ^-,p) Elastic Scattering*

H. A. RUBIN†‡
University of Maryland, College Park, Maryland

AND

R. A. BURNSTEIN
Illinois Institute of Technology, Chicago, Illinois

(Received 16 February 1967)

The cross sections for the elastic scattering of Σ^+ and Σ^- hyperons on protons have been measured. The hyperons were produced by the interactions of stopping K^- mesons in a hydrogen bubble chamber. The cross section for (Σ^-,p) elastic scattering is 166±33 mb, at a mean laboratory momentum of 150 MeV/c. The cross section for (Σ^+,p) elastic scattering is 84±34 mb at a mean laboratory momentum of 161.5 MeV/c. These measurements, as well as the results of similar experiments, are compared with several recent theoretical predictions of hyperon-nucleon scattering cross sections.

I. INTRODUCTION

In the last few years theoretical studies of hyperon nucleon interactions have been made by a number of authors using different approaches.[1–4] Much of the experimental data available has been of an indirect nature–originating from the analysis of hyperfragment systems.[5] Recently, however, direct measurements have been made of two-body hyperon-proton systems.[6–8] In this paper, we report the direct measurement of (Σ^+,p) and (Σ^-,p) elastic scattering in a hydrogen bubble chamber and compare these results with some recent theoretical predictions. Section II describes the experimental procedure; Sec. III presents the results for $\sigma_{el}(\Sigma^+,p)$ and $\sigma_{el}(\Sigma^-,p)$; and Sec. IV contains some discussion and conclusions.

II. EXPERIMENTAL PROCEDURE

The Σ^+ and Σ^- hyperons, which were the subject of this study, were produced by the interactions of a beam of stopping K^- mesons[9] in the Saclay 81-cm hydrogen bubble chamber[10] at CERN. The reactions producing $\Sigma^\pm$ hyperons are:

$$K^-+p\rightarrow\Sigma^++\pi^- \quad (1a)$$

$$K^-+p\rightarrow\Sigma^-+\pi^+. \quad (1b)$$

* Supported in part by U. S. Atomic Energy Commission Contract No. AT-(40-1)-2540.

† Present address: Illinois Institute of Technology, Chicago, Illinois.

‡ This paper forms the subject of a thesis submitted in partial fulfillment of the requirements for the degree of Doctor of Philosophy, University of Maryland, 1967 [University of Maryland Technical Report No. 652 (unpublished)].

[1] P. D. De Souza, G. A. Snow and S. Meshkov, Phys. Rev. **135**, B565 (1964); and P. D. De Souza, University of Maryland Technical Report No. 565, 1965 (unpublished).

[2] S. Iwao, Nuovo Cimento **34**, 1167 (1964).

[3] J. C. Helder and J. J. de Swart, Phys. Letters **21**, 109 (1966).

[4] Y. C. Tang and R. C. Herndon, Phys. Rev. **151**, 1116 (1966).

[5] For a recent review article see R. H. Dalitz, Conference on the Use of Elementary Particles in Nuclear Structure Research, September 1965 (unpublished) and references contained therein.

[6] R. A. Burnstein, University of Maryland Technical Report No. 469, 1965 (unpublished).

[7] G. Alexander *et al.*, Phys. Letters **19**, 715 (1966); and B. Sechi-Zorn, R. A. Burnstein, B. Kehoe, and G. Twitty (to be published).

[8] H. G. Dosch, R. Engelmann, H. Filthuth, V. Hepp. *et al.*, Phys. Letters **21**, 236 (1966); **21**, 236 (1966).

[9] A description of the beam is given by B. Aubert, H. Courant, H. Filthuth, A. Segar, and W. Willis, Nucl. Instr. Methods **20**, 51 (1963).

[10] P. Baillon, thesis, University of Paris 1963 (unpublished).